frontiers | Frontiers in Physics

ORIGINAL RESEARCH
published: 01 June 2022
doi: 10.3389/fphy.2022.915266

All-Fiber Wideband Supercontinuum Generation in Short Hybrid Highly Nonlinear Fibers With a Femtosecond Erbium-Doped Fiber Laser

Shuang Zhang[1], *Hao Qiao*[1], *Tao Zhang*[1], *Min Zhou*[1]* *and Xinye Xu*[1,2]*

[1]State Key Laboratory of Precision Spectroscopy, East China Normal University, Shanghai, China, [2]Shanghai Research Center for Quantum Sciences, Shanghai, China

Wideband supercontinuum (SC) generation has attracted considerable attention due to its various practical applications in many fields. We report on all-fiber SC generation in hybrid highly nonlinear fibers (HNLFs) pumped with a femtosecond erbium-doped fiber laser (EDFL). Based on the nonlinear polarization rotation (NPR) technique, the EDFL is compactly constructed with a hybrid device integrating a wavelength-division multiplexing (WDM) coupler, a tap coupler, and a polarization-sensitive isolator. The SC emission in HNLFs with different dispersions is characterized and the optimum length of HNLF is found. The SC in the hybrid HNLF, constructed by two sections of HNLFs with positive and zero dispersions, could approximately span an octave spanning in the 20 dB bandwidth. Our system suggests an inexpensive, effective and compact construction for SC generation.

Keywords: ultrashort pulse, supercontinuum generation, highly nonlinear fiber, group velocity dispersion, hybrid fiber

OPEN ACCESS

Edited by:
Venugopal Rao Soma,
University of Hyderabad, India

Reviewed by:
Dong Mao,
Northwestern Polytechnical University, China
Haifeng Jiang,
University of Science and Technology of China, China

Correspondence:
Xinye Xu
xyxu@phy.ecnu.edu.cn
Min Zhou
mzhou@lps.ecnu.edu.cn

Specialty section:
This article was submitted to Optics and Photonics, a section of the journal Frontiers in Physics

Received: *07 April 2022*
Accepted: *12 May 2022*
Published: *01 June 2022*

Citation:
Zhang S, Qiao H, Zhang T, Zhou M and Xu X (2022) All-Fiber Wideband Supercontinuum Generation in Short Hybrid Highly Nonlinear Fibers With a Femtosecond Erbium-Doped Fiber Laser. Front. Phys. 10:915266. doi: 10.3389/fphy.2022.915266

INTRODUCTION

Over the past few decades, supercontinuum (SC) generation has stimulated extensive research on optical coherence tomography, micromachining, nonlinear frequency conversion, light detection and ranging (LIDAR), and the optical frequency comb [1–5]. Since Alfano and Shapiro first observed the spectrum spanning 400–700 nm in bulk glasses in 1970, much attention has been paid to developing broadband and easy-to-use SC light sources [6]. Thanks to advances in fiber technology, SC generation nowadays has been widely exploited in specially manufactured optical fibers, such as micro-structured photonic crystal fibers (PCFs), tapered fibers, and highly nonlinear fibers (HNLFs) [7–9]. SC light sources are available to span a spectral range over hundreds of nanometers and allow for high temporal coherence as well.

SC generation occurs when ultrashort optical pulses propagate through the nonlinear fiber. Only when the launching pulse power is larger than the threshold of the SC spectrum, the significant spectrum broadening phenomenon can be observed [10–12]. At present, various passive mode-locking techniques are used to generate stable femtosecond pulses, such as nonlinear polarization rotation (NPR) [13–15], nonlinear amplifying loop mirror [16–18], and saturable absorbers [19–22]. The source energy can be easily boosted to a few nJ with the fiber amplifier, which generally satisfies the required condition for SC generation. The laser energy within the optical fiber is limited to a smaller core of the waveguide than the bulk medium. The resulting high-power density is conducive to getting nonlinear optical effects. A large number of nonlinear effects contribute the spectral

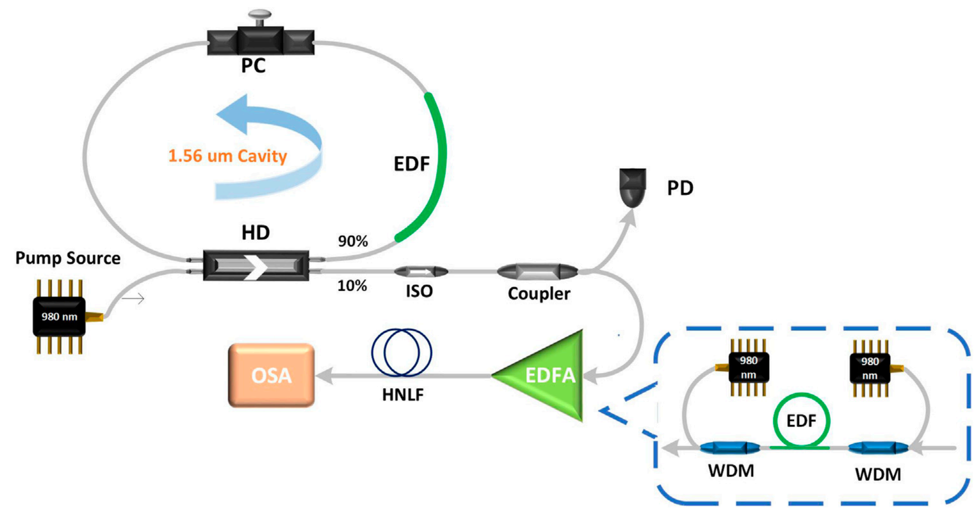

FIGURE 1 | Experimental schematic of the SC generation using a passively mode-locked femtosecond EDFL. The dispersion compensation fibers are not depicted. HD: hybrid device, comprising a wavelength-division multiplexing (WDM) coupler, a tap coupler, and a polarization-sensitive isolator, EDF: erbium-doped fiber, PD: photodiode detector, PC: polarization controller, ISO: optical isolator, HNLF: highly nonlinear fiber, OSA: optical spectrum analyzer.

broadening, including self-phase modulation (SPM), cross-phase modulation (XPM), stimulated Raman scattering, four-wave mixing and other high-order nonlinear effects [17]. Moreover, these nonlinear contributions are strongly related to the group velocity dispersion (GVD) and the length of the optical fiber, besides the power and the duration of the pulsed source.

As mentioned above, the HNLF is one kind of the most commonly used fibers for generating the SC spectrum. A combination of the HNLF and the femtosecond erbium-doped fiber laser (EDFL) can generate the SC spectrum around 1.55 μm. The HNLF enhances the fiber nonlinearity mainly in two aspects: its silica core is doped with a high concentration of germanium dioxide (GeO_2), and the core diameter is made as small as several nanometers [23]. Thus, the nonlinear coefficient γ (typically 10–20 W^{-1} km^{-1}) of HNLFs is several times larger than that of the standard single-mode fiber (SSMF). Although it is smaller than γ of the PCFs, HNLFs can be conveniently fusion spliced to other fibers with negligible losses (e.g, <0.2 dB for sliced to the SSMF), which is beneficial to construct all-fiber SC systems. Additionally, the HNLF has low propagation loss and can be manufactured with a low dispersion slope.

It is well known that control of SC generation requires fine lengthwise management of HNLF parameters, i.e., dispersion management. In the normal GVD regime, tens meters of conventional HNLFs are commonly used to extend the spectral continuum over an octave (i.e., 1–2 μm) [24, 25]. For example, Gao *et al.* reported an all-fiber SC source spanning 1120–2245 nm in the 10 dB bandwidth with a 20-m long HNLF [24]. In the anomalous GVD regime, the HNLF length for wide SC generation can be essentially shortened to a few meters [26, 27]. It is worth noting that Nicholson *et al.* accessed the feasibility of broadening the continuum by splicing sections of different-dispersion HNLF together [27, 28]. To further relax the length requirement for practical applications, many studies elaborately tested the hybrid HNLF constructed from plural sections [29–32]. Hori *et al.* presented a continuum spanning about 1000 nm by injecting the ultrashort pulse into the anomalous GVD near the zero-dispersion wavelength (ZDW) of the HNLF [29]. Korel *et al.* demonstrated the SC generation over 1–2 μm in a hybrid HNLF with the length of tens centimeter [32].

In this paper, we present a simple, compact, and inexpensive experimental system for wideband SC generation. The system consists of all non-polarization-maintaining (non-PM) fibers and off-the-shelf optical devices. Additionally, the nonlinear coefficient γ of our HNLFs is 10 W^{-1} km^{-1}, one half γ of specially-made HNLFs in many works [27]. We study a short-length dispersion-managed hybrid HNLF pumped by a mode-locked fiber laser to generate the SC spectrum. By changing the length of sectional HNLF and the peak power of the ultra-short pulse laser, the effects on the continuum are studied. A hybrid HNLF consisting of two sections, with a total length of less than 1 m, is finally selected to generate an octave SC spectrum.

EXPERIMENTAL SETUP

A schematic of the SC generation system is shown in **Figure 1**. The all-fiber laser is a stretched-pulse ring oscillator employing NPR as the mode-locking mechanism [33]. The cavity is made of an erbium-doped fiber (OFS EDF80), one segment of SSMF, a polarization controller and a hybrid three-in-one device. The hybrid device integrates a wavelength-division multiplexer (WDM) coupler, a 10% output coupler, and a polarization-sensitive optical isolator. Using such a hybrid device allows us

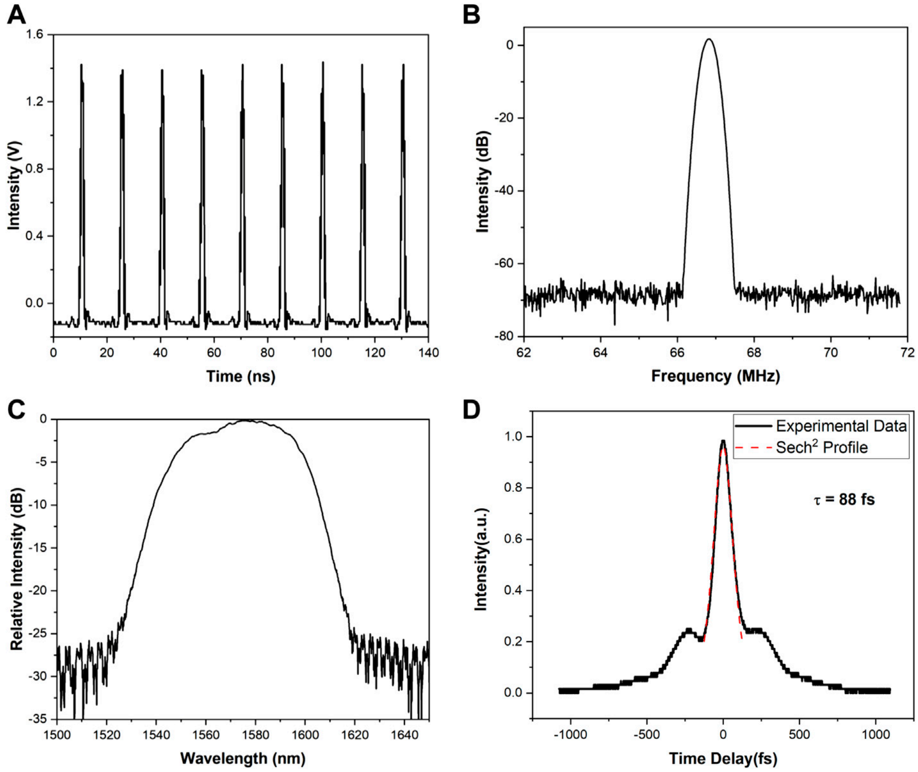

FIGURE 2 | Output of the fiber laser when the mode-locked mechanism is self-started: **(A)**. pulse trains, **(B)**. rf spectrum with the fundamental rate. The resolution bandwidth (RBW) of the rf spectrum is 300 kHz. **(C)** Optical spectrum. The RBW of the optical spectrum is 0.15 nm. **(D)** The autocorrelation trace of amplified pulses before coupled into the HNLF. The trace center is fitted with sech^2 function, showing a full width half maximum (FWHM) pulse width of 88 fs.

to reduce the number of elements in the cavity and therefore make the oscillator compact. The GVD coefficients β_2 of the EDF80 and SSMF at 1550 nm are +61.2 ps^2/km (anomalous dispersion) and −22.9 ps^2/km (normal dispersion), respectively. The net group delay dispersion (GDD) of the oscillator is estimated to be 0.0025 ps^2 ± 0.0054 ps^2. The ring oscillator is forward pumped by a laser diode at 980 nm. When the polarization controller is properly adjusted, mode-locking is obtained and can be self-starting. At 141 mW of pump power, 3.9 mW of average output power at 1570 nm at a fundamental rate of 66.83 MHz is generated.

The output pulses are stretched with a 4 m length of normal-dispersion fiber (DCF38), whose β_2 is +48.8 ps^2/km at 1550 nm. Then, the power of the oscillator pulse is boosted by using the erbium-doped fiber amplifier (EDFA). The 1.35 m of active EDF (Er110) is pumped bidirectionally with two 980-nm diode lasers through two WDM couplers, and β_2 for Er110 is +12 ps^2/km. After the pulse is broadened and amplified, a segment of SSMF is used in the compression stage, whose β_2 is opposite to that of DCF38.

The EDFA output pulse is recompressed using a section of SSMF, and then enters into the HNLF for SC generation. The radiation generated in the HNLF is acquired for spectral measurements directly at the HNLF end. The laser spectrum is recorded with a mid-infrared fiber optic analyzer. It can collect spectral data over the range from 1 to 3.4 μm with resolution of 0.15 nm. The analyzer calibration is based on an infrared laser at the known wavelength of 1156 nm. An autocorrelator is used to measure the laser pulse width. The rf spectra are measured with an rf spectrum analyzer (Rigol DSA815).

RESULTS AND DISCUSSION

EDFL and Amplified Pulse Characterization

Figure 2A shows the pulse train with the oscillator working in the mode-locking state. The pulse-to-pulse separation is about 15.00 ns, which corresponds to a repetition frequency of 66.83 MHz. As shown in **Figure 2B**, the rf spectrum also clearly reveals this fundamental rate, and it appears a signal-to-noise ratio (SNR) of 70 dB. **Figure 2C** shows the optical spectrum, where the 3 dB bandwidth is estimated to be 46.7 nm. Characteristics of a single-peak autocorrelation trace, no oscillation in the optical spectrum, and a clear pulse train confirm that the EDFL is stably operated in the single-pulse mode-locking state. As shown in **Figure 2D**, amplified pulses are obtained with the narrowest width of 88 fs and the average power of 140 mW, corresponding to the pulse peak power of 23.3 kW. There is a base at the edge of the pulse on both sides. It is due to the high power density and strong nonlinear effects of the pulse transmitting in the fiber, which affect the pulse shape after the transmission through the longer fiber.

TABLE 1 | Parameters of the HNLFs used in the experiments.

Type	Cutoff wavelength (nm)	MFD (μm)	Dispersion@1550 nm (ps/nm/km)	Dispersion Slope@1550 nm (ps/nm^2/km))	Attenuation @1550 nm (dB)	Typical nonlinear coefficient (W^{-1}km^{-1})
NEG	1215	3.78	−3.990	0.006	0.885	10
ZERO	1274	3.80	−0.220	0.019	0.900	10
POS	1274	3.81	1.477	0.019	0.876	10
POS	1357	4.02	3.139	0.020	1.129	10
POS	1399	4.00	4.205	0.017	1.120	10
POS	1348	4.24	5.272	0.034	0.796	10

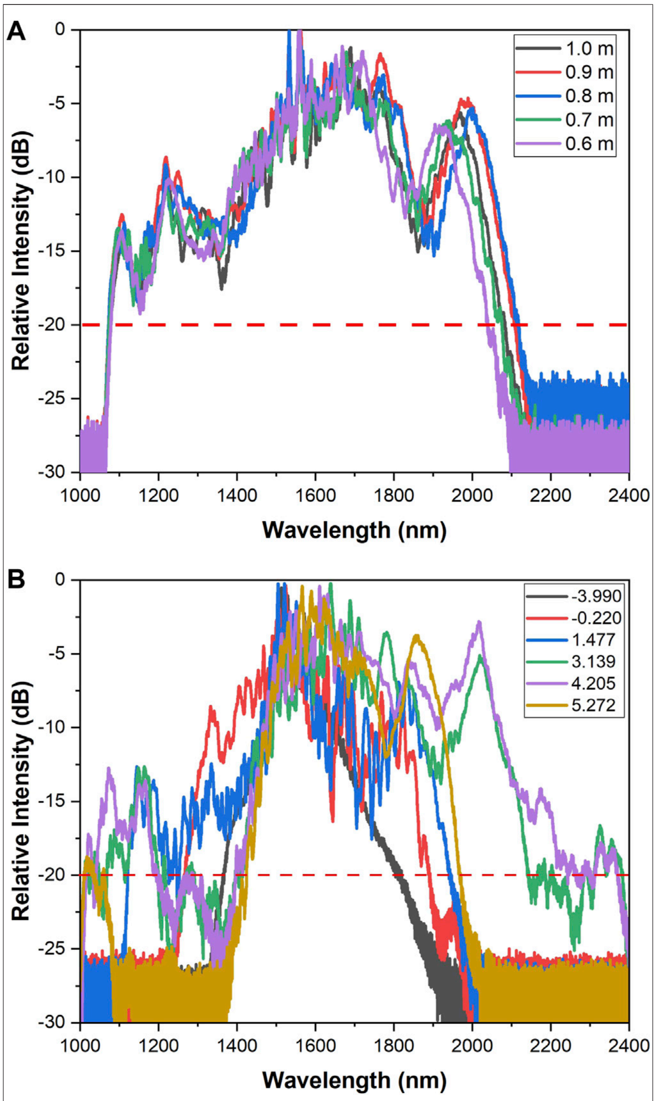

FIGURE 3 | (A) SC spectra in the HNLF with D = 3.139 ps/nm/km by changing the HNLF length. **(B)** SC spectra in a 0.8-m-long HNLF with respect to different dispersions.

SC Generation in HNLF With Different Dispersions

In general, to generate an SC spectrum with the HNLF, the pulse energy is required more than 1 nJ, which is specially designed from a 1550 nm pulse laser source [25]. After amplified by EDFA, the average power of the pulse is 140 mW, and the peak power of the pulses increases with the decrease of the pulse width. In the follow-up study of the effect of the HNLFs, we chose amplified pulses with the narrowest width of 88 fs before sent into HNLF. In our experiments, the HNLFs have dispersion parameters D ranging from −3.990 to 5.272 ps/nm/km at 1550 nm. Other parameters of HNLF are shown in **Table 1**.

Usually, when pumping in the anomalous dispersion region, the splitting of the higher-order soliton can promote the generation of SCs, but have relatively low coherence [34, 35]. In contrast, when pumping in the normal dispersion region, the spectral broadening is devoted by SPM and optical wave breaking (OWB), and the SC spectrum is flat and has good coherence [7, 36]. But in the experiment, it is also necessary to consider the dispersion and the width of the pulse to select the HNLF. We investigate the generation of SC by using HNLF with different dispersion values D under fixed pump pulse parameters.

Here, the HNLF with one kind dispersion is used for generating the SC, as shown in **Figure 3**. By using the HNLF with D = 3.139 ps/nm/km and varying the length of the fiber from 0.6 to 1.0 m, we observe corresponding SC spectra as shown in **Figure 3A**. The spectral range of SC does not monotonously increase with the extended length of HNLF. It is found that 0.8 m is the optimum length when the length of fiber is required to be less than 1 m. Similarly, the generated continua in the 0.8-m-long HNLF with different dispersions are shown in **Figure 3B**. The wideband SC extending from 1010 to 2400 nm over an octave spanning is generated, and at the 20 dB bandwidth, a broadening range of 1050–2230 nm is observed in the case of D = 4.205 ps/nm/km. As the HNLF dispersion increases, the output spectrum starts broadening on both sides. The spectral range gradually increases due to the accumulation of nonlinear effects, but the spectral coherence becomes worse, and the intensity decreases significantly at 1200–1400 nm. It appears the spectral fine structure, which is the results of this XPM effect and the interference between the components which are spectrally overlapped but are temporally separated.

Besides, it should be noted that the mid-infrared fiber optic analyzer has a wide measurement range from 1 μm to 3.4 μm. But we are mainly concerned with the case that the center wavelength 1570 nm pulse is broadened to an octave SC, so the spectral range is focused between 1–2.4 μm.

As the peak power of the pump changes, the width of the SC also changes significantly. We choose the 0.8 m length of HNLF with D = 4.205 ps/nm/km. When the peak power is increased

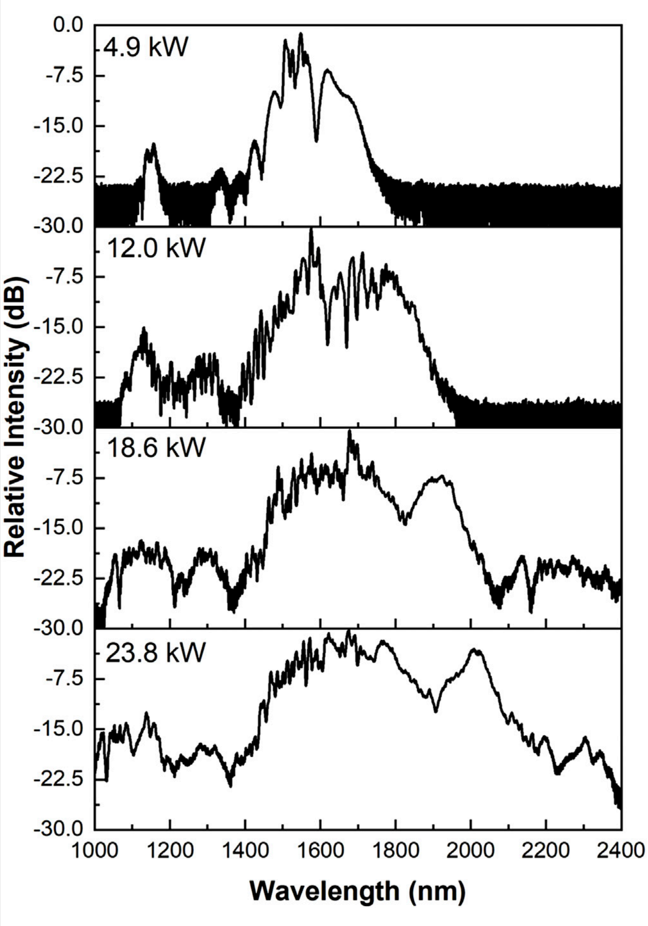

FIGURE 4 | SC spectra in a 0.8-m-long HNLF with D = 4.205 ps/nm/km at 1550 nm as a function of the peak power.

from 4.9 to 23.8 kW, it can be seen from **Figure 4** that the wavelength of the SC is significantly wider, especially in the long-wavelength band. This is mainly because with the increase of the peak power of the pump, the depletion time of the pump is prolonged, the propagation distance is longer, and the nonlinear effects such as SPM are significantly enhanced. At the max available peak power of 23.8 kW (~140 mW of averaging power), the spectrum can be broadened from 1010 nm to 2230 nm in the 20 dB bandwidth.

SC Generation in a Hybrid HNLF

In this section, we study the effect of the hybrid HNLF with different dispersions on the continuum. We splice together two types of highly nonlinear fibers, and the splicing loss of these two fibers is less than 0.6 dB/splice. We find that the HNLF with negative dispersion has little influence on spectral broadening. So just HNLFs with zero and positive dispersion are considered. We construct the hybrid HNLF consisting of only two sections of HNLFs, and the total positive dispersion can be realized in two fusion spliced manners: between HNLFs with positive and negative dispersion, and between HNLFs with positive and zero dispersion.

Firstly, the SC is generated in a hybrid HNLF constructed by two HNLFs with 0.6 m positive dispersion and 0.2 m zero dispersion, where the positive dispersion is D = 4.205 ps/nm/km. We make comparison of the SC spectra measured with uniform and hybrid nonlinear fibers for three cases: in the hybrid HNLF with a total length of 0.8 m, in the 0.6 m HNLF, and in the 0.8 m HNLF. SC generation in the hybrid HNLF is noticeably more efficient. **Figure 5** shows the typical spectral broadening in uniform and hybrid HNLF. Distinctly, the SC spectrum generated in the hybrid HNLF is much broader in the 20 dB bandwidth. The primary spectral broadening is caused in the first stage of HNLF-POS. The higher peak power and the narrower temporal duration produce the widely broadened SC spectrum. However, the spectrum has several discrete peaks and the flatness becomes to be degraded. The ZDW of HNLF-ZERO is 1550 nm and it is almost matched with the pump wavelength of 1570 nm. Through the second section of this hybrid HNLF, it continues accumulating nonlinear effects of the transmitting pulse and increases the intensity of each component of the SC, especially from 1250 nm to 1450 nm.

Two sections of HNLFs with D = 3.139 ps/nm/km and D = 5.272 ps/nm/km are used to construct the second hybrid HNLF for comparison. To demonstrate the effectiveness of this hybrid HNLF, we compare the spectra generated by the hybrid HNLF and the 0.8 m uniform HNLF with D = 4.205 ps/nm/km. We make both the total GDD and the length of the hybrid HNLF close to the uniform HNLF. The hybrid HNLF is constructed by a 0.4 m length of HNLF with D = 3.139 ps/nm/km and a 0.4 m length of HNLF with D = 5.272 ps/nm/km. As shown in **Figure 6**, the spectrum generated by the hybrid HNLF is much broader, i.e., in the wavelength range of 2000–2100 nm. The effect of the hybrid fiber obtained by

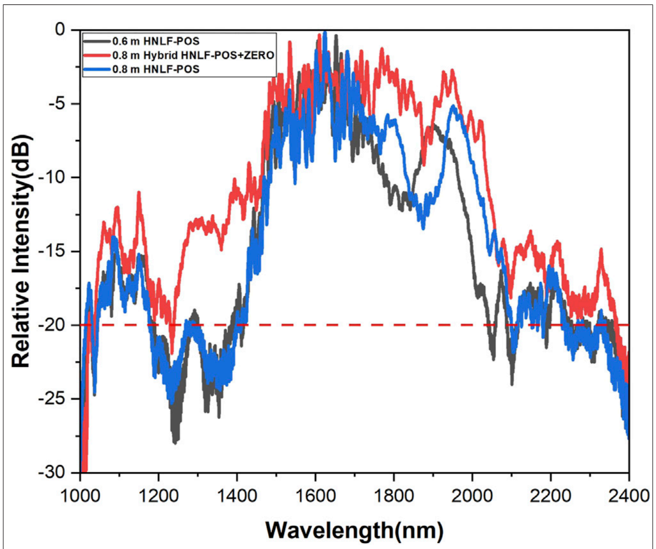

FIGURE 5 | The spectra generated in the HNLFs and the hybrid HNLF. The black line and blue line represent the 0.6 m and 0.8 m-long HNLFs with D = 4.205 ps/nm/km, respectively. The red line represents the hybrid HNLF consisting of two sections of HNLFs with D = 4.205 ps/nm/km (0.6 m) and zero dispersion (0.2 m).

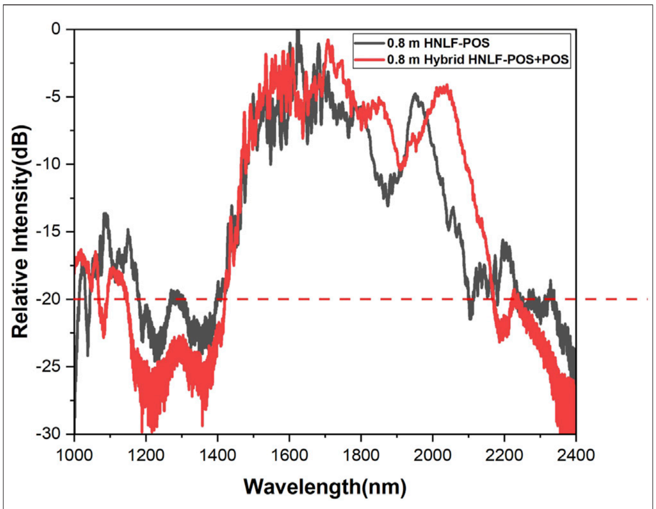

FIGURE 6 | The spectra generated in the HNLF and the hybrid HNLF. The red line is an SC generated by the hybrid HNLF with two different positive dispersion. The total GDD is close to that in the 0.8 m HNLF with D = 4.205 ps/nm/km.

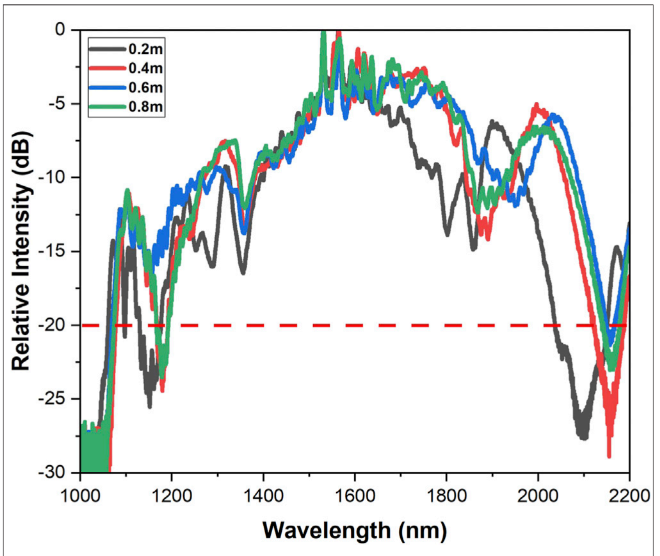

FIGURE 8 | The SC is generated in the hybrid HNLF with 0.2 m zero dispersion and positive dispersion fiber of varying length.

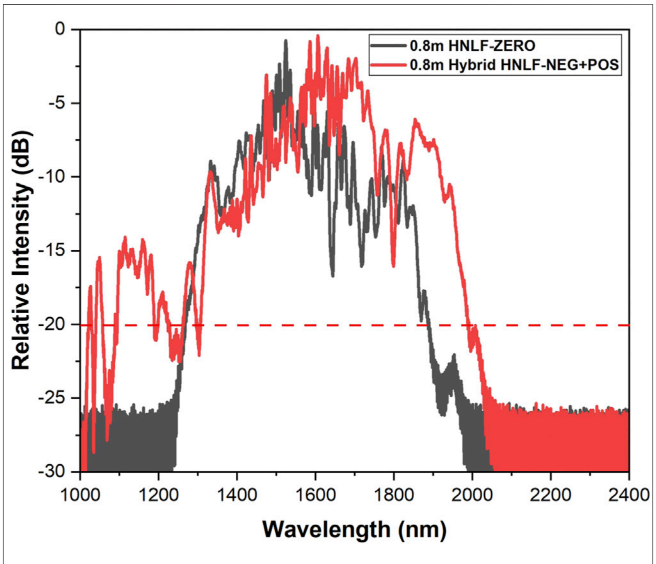

FIGURE 7 | Comparing the spectra generated by the 0.8 m HNLF with zero dispersion (black line) and the hybrid HNLF with positive and negative dispersion (red line).

splicing different positive dispersion of HNLFs has not much difference from that of the uniform HNLF. Additionally, due to the limitation of the measurement range of the spectrometer, it is inconvenient to compare spectra with wavelengths less than 1000 nm.

Then, we splice a 0.43 m HNLF with D = 4.205 ps/nm/km and a 0.37 m HNLF with D = -3.990 ps/nm/km to construct another hybrid HNLF. **Figure 7** describes the spectra generated by the hybrid HNLF and the 0.8 m HNLF with zero dispersion, and the spectral broadening generated by the hybrid HNLF is wider distinctly. Splicing a positive dispersion HNLF and a negative-positive dispersion HNLF together is beneficial to the continuum on both sides. SC expands broadly through the normal dispersion region of the HNLF firstly, and in the anomalous dispersion region of the fiber, the SC spectrum would be flat and have a better coherence than the spectrum by uniform HNLF-ZERO. Although this type of hybrid HNLF has better broadening effect than the uniform fiber, it has unobtrusive effect on long wavelength components of SC due to the alternation of positive and negative dispersion.

Based on the above results, it shows that the hybrid HNLF constructed from sectional HNLFs with zero and positive dispersion has a better effect on the SC than the other two types of hybrid HNLFs. Further, we try to shorten the total length of HNLF to improve the stability and reduce the cost of the system. The length of the HNLF with zero dispersion is fixed at 0.2 m, and the length of the positive dispersion (D = 4.205 ps/nm/km) HNLF is changed from 0.2 to 0.8 m. The obtained spectra are shown in **Figure 8**. In the range of 1150–1250 nm, the spectrum generated in the hybrid HNLF with 0.6 m length of positive dispersion is slightly intense. It also shows that shortening the length of the hybrid HNLF is not always favorable for the broadening of the SC spectrum.

CONCLUSION

In summary, we have demonstrated wide SC generation in the hybrid HNLF with different dispersions using passively NPR-based mode-locked EDFL. A pulse train is generated with a repetition frequency of 66.83 MHz and the 3 dB bandwidth of the spectrum is 46.7 nm at the center wavelength of 1570 nm. The SC covering a range of 1020–2230 nm in the 20 dB bandwidth is achieved using an HNLF with uniform D =

4.205 ps/nm/km. The length of the HNLF and the launching pulse power are then studied. We find that the optimum length is 0.8 m in this system. Just two segments of HNLF are spliced together to construct the hybrid HNLF. It is found that SC generation in the hybrid fiber with positive and zero dispersions has a preferable spectral intensity, and the broadening range almost spans an octave in the 20 dB bandwidth. Our scheme of using the hybrid HNLF in SC generation is a good example that matches an arbitrary pumping pulse source, and suggests an inexpensive, effective, and compact construction for SC generation.

DATA AVAILABILITY STATEMENT

The original contributions presented in the study are included in the article/Supplementary material, further inquiries can be directed to the corresponding authors.

AUTHOR CONTRIBUTIONS

SZ, MZ, and XX proposed the idea. SZ, HQ, and TZ performed the experiments. SZ wrote the original manuscript. HQ, TZ, MZ, and XX revised the manuscript. All authors contributed to the article and approved the submitted version. XX supervised the project.

FUNDING

This work is supported by National Natural Science Foundation of China under Grant Nos. 62105102 and 11134003, National Key Research and Development Program of China under Grant Nos. 2016YFA0302103, 2017YFF0212003, and 2016YFB0501601, Shanghai Municipal Science and Technology Major Project under No. 2019SHZDZX01, Shanghai Excellent Academic Leaders Program under No. 12XD1402400.

REFERENCES

1. Jacek S, Maria M, Gwenael M. Mid-IR Supercontinuum Generation in a ZBLAN Fiber Pumped by a Gain-Switched Mode-Locked Tm-Doped Fiber Laser and Amplifier System. *Opt Express* (2013) 21(7):7851–7. doi:10.1364/OE.21.007851
2. Kivanç Ö, Bülent Ö, Sinem Y, Ömer FI, Koray E. 83 W, 3.1 MHz, Square-Shaped, 1 Ns-Pulsed All-Fiber-Integrated Laser for Micromachining. *Opt Express* (2011) 19(18):17647–52. doi:10.1364/OE.19.017647
3. Sergey VS, Sergey MK, Sergey VK. Efficiency of Non-linear Frequency Conversion of Double-Scale Pico-Femtosecond Pulses of Passively Mode-Locked Fiber Laser. *Opt Express* (2014) 22(1):1058–64. doi:10.1364/OE.22.001058
4. Chen Y, Räikkönen E, Kaasalainen S, Suomalainen J, Hakala T, Hyyppä J, et al. Two-channel Hyperspectral LiDAR with a Supercontinuum Laser Source. *Sensors* (2010) 10(7):7057–66. doi:10.3390/s100707057
5. Udem T, Holzwarth R, Hänsch T. Femtosecond Optical Frequency combs. *Eur Phys J Spec Top* (2009) 172(1):69–79. doi:10.1140/epjst/e2009-01042-6
6. Alfano RR, Shapiro SL. Emission in the Region 4000 to 7000 Å *via* Four-Photon Coupling in Glass. *Phys Rev Lett* (1970) 24(11):584–7. doi:10.1103/physrevlett.24.584
7. Dudley JM, Genty G, Coen S. Supercontinuum Generation in Photonic crystal Fiber. *Rev Mod Phys* (2006) 78(4):1135–84. doi:10.1103/RevModPhys.78.1135
8. Birks TA, Wadsworth WJ, Russell PSJ. Supercontinuum Generation in Tapered Fibers. *Opt Lett* (2000) 25(19):1415–22. doi:10.1364/ol.25.001415
9. Nishizawa N, Goto T. Widely Broadened Super Continuum Generation Using Highly Nonlinear Dispersion Shifted Fibers and Femtosecond Fiber Laser. *Jpn J Appl Phys* (2001) 40:L365–L367. doi:10.1143/jjap.40.l365
10. Alfano RR, Shapiro SL. Observation of Self-phase Modulation and Small-Scale Filaments in Crystals and Glasses. *Phys Rev Lett* (1970) 24(11):592–4. doi:10.1103/physrevlett.24.592
11. Mori K, Takara H, Kawanishi S, Saruwatari M, Morioka T. Flatly Broadened Supercontinuum Spectrum Generated in a Dispersion Decreasing Fibre with Convex Dispersion Profile. *Electron Lett* (1997) 33(21):1806–8. doi:10.1049/el:19971184
12. Okuno T, Onishi M, Nishimura M. Generation of Ultra-broad-band Supercontinuum by Dispersion-Flattened and Decreasing Fiber. *IEEE Photon Technol Lett* (1998) 10(1):72–4. doi:10.1109/68.651109
13. Hofer M, Ober MH, Haberl F, Fermann ME. Characterization of Ultrashort Pulse Formation in Passively Mode-Locked Fiber Lasers. *IEEE J Quan Electron.* (1992) 28(3):720–8. doi:10.1109/3.124997
14. Fermann ME, Stock ML, Andrejco MJ, Silberberg Y. Passive Mode Locking by Using Nonlinear Polarization Evolution in a Polarization-Maintaining Erbium-Doped Fiber. *Opt Lett* (1993) 18(11):894–6. doi:10.1364/ol.18.000894
15. Tamura K, Haus HA, Ippen EP. Self-starting Additive Pulse Mode-Locked Erbium Fibre Ring Laser. *Electron Lett* (1992) 28(24):2226–8. doi:10.1049/el:19921430
16. Duling IN. All-fiber Ring Soliton Laser Mode Locked with a Nonlinear Mirror. *Opt Lett* (1991) 16(8):539–41. doi:10.1364/ol.16.000539
17. Richardson DJ, Laming RI, Payne DN, Matsas V, Phillips MW. Selfstarting, Passively Modelocked Erbium Fibre Ring Laser Based on the Amplifying Sagnac Switch. *Electron Lett* (1991) 27(6):542–4. doi:10.1049/el:19910341
18. Wong WS, Namiki S, Margalit M, Haus HA, Ippen EP. Self-switching of Optical Pulses in Dispersion-Imbalanced Nonlinear Loop Mirrors. *Opt Lett* (1997) 22(15):1150–2. doi:10.1364/ol.22.001150
19. Polynkin A, Polynkin P, Panasenko D, Mansuripur M, Moloney J, Peyghambarian N. Short-cavity, Passively Modelocked Fibre Laser Oscillator at 1.5 [micro Sign]m with 550 MHz Repetition Rate and High Average Power. *Electron Lett* (2006) 42(3):157–9. doi:10.1049/el:20063878
20. Chong A, Renninger WH, Wise FW. Environmentally Stable all-normal-dispersion Femtosecond Fiber Laser. *Opt Lett* (2008) 33(10):1071–3. doi:10.1364/ol.33.001071
21. Olsson RK, Andersen TV, Leick L, Levitan V, Jepsen PU, Turchinovich D. *All-polarization-maintaining Yb Laser Delivering 13 nJ Pulses Compressible to 140 fs. Poster Session Presented at NanoDay*. Denmark: Kgs. Lyngby (2007).
22. Mao D, Wang H, Zhang H, Zeng C, Du Y, He Z, et al. Synchronized Multi-Wavelength Soliton Fiber Laser *via* Intracavity Group Delay Modulation. *Nat Commun* (2021) 12:6712–9. doi:10.1038/s41467-021-26872-x
23. Okuno T, Onishi M, Kashiwada T, Ishikawa S, Nishimura M. Silica-based Functional Fibers with Enhanced Nonlinearity and Their Applications. *IEEE J Select Top Quan Electron.* (1999) 5(5):1385–91. doi:10.1109/2944.806765
24. Gao W, Liao M, Yang L, Yan X, Suzuki T, Ohishi Y. All-fiber Broadband Supercontinuum Source with High Efficiency in a Step-index High Nonlinear Silica Fiber. *Appl Opt* (2012) 51(8):1071–5. doi:10.1364/ao.51.001071
25. Zhu S, Liu D, Tang M, Fu S, Zhao L. Supercontinuum Generation with a Repetition Rate over 100MHz Based on a Picosecond Pulse from a normal Dispersion Fiber Laser. In: Proceeding of the 15th Int Conf on Optical Communications and Networks (ICOCN); Sept. 2016; Hangzhou, China. IEEE (2016). p. 1–3. doi:10.1109/ICOCN.2016.7921046
26. Nishizawa N, Goto T. Widely Broadened Super Continuum Generation Using Highly Nonlinear Dispersion Shifted Fibers and Femtosecond Fiber Laser. *Jpn J Appl Phys* (2001) 40(4B):L365–L367. doi:10.1143/jjap.40.l365
27. Nicholson JW, Yan MF, Wisk P, Fleming J, DiMarcello F, Monberg E, et al. All-fiber, Octave-Spanning Supercontinuum. *Opt Lett* (2003) 28(8):643–5. doi:10.1364/ol.28.000643
28. Nicholson JW, Abeeluck AK, Headley C, Yan MF, Jrgensen CG. Pulsed and Continuous-Wave Supercontinuum Generation in Highly Nonlinear, Dispersion-Shifted Fibers. *Appl Phys B* (2003) 77(2):211–8. doi:10.1007/s00340-003-1201-z

29. Hori T, Takayanagi J, Nishizawa N, Goto T. Flatly Broadened, Wideband and Low Noise Supercontinuum Generation in Highly Nonlinear Hybrid Fiber. *Opt Express* (2004) 12(2):317–24. doi:10.1364/opex.12.000317
30. Bagaev SN, Denisov VI, Dianov EM, Korel' II, Kuznetsov SA, Pivtsov VS, et al. Spectral Broadening of Radiation from a Femtosecond Cr:forsterite Laser in Highly Nonlinear Fibers. *J Exp Theor Phys* (2007) 105(5):881–5. doi:10.1134/s1063776107110015
31. Kobtsev SM, Smirnov SV. Fiber Supercontinuum Generators with an Extended Set of Controlled Parameters in Real Time Scale. *Opt Spectrosc* (2009) 107: 339–43. doi:10.1134/s0030400x09090033
32. Korel II, Nyushkov BN, Denisov VI, Pivtsov VS, Koliada NA, Sysoliatin AA, et al. Hybrid Highly Nonlinear Fiber for Spectral Supercontinuum Generation in mobile Femtosecond Clockwork. *Laser Phys* (2014) 24(7):074012. doi:10. 1088/1054-660x/24/7/074012
33. Tamura K, Ippen EP, Haus HA, Nelson LE. 77-fs Pulse Generation from a Stretched-Pulse Mode-Locked All-Fiber Ring Laser. *Opt Lett* (1993) 18(13): 1080–2. doi:10.1364/ol.18.001080
34. Abeeluck AK, Headley C. Continuous-wave Pumping in the Anomalous- and normal-dispersion Regimes of Nonlinear Fibers for Supercontinuum Generation. *Opt Lett* (2005) 30:61–3. doi:10.1364/ol.30.000061
35. Gattass RR, Brandon Shaw L, Nguyen VQ, Pureza PC, Aggarwal ID, Sanghera JS. All-fiber Chalcogenide-Based Mid-infrared Supercontinuum Source. *Opt Fiber Tech* (2012) 18:345–8. doi:10.1016/j.yofte.2012.07.003
36. Kedenburg S, Strutynski C, Kibler B, Froidevaux P, Désévédavy F, Gadret G, et al. High Repetition Rate Mid-infrared Supercontinuum Generation from 13 to 53 μm in Robust Step-index Tellurite Fibers. *J Opt Soc Am B* (2017) 34:601–7. doi:10. 1364/josab.34.000601

Conflict of Interest: The authors declare that the research was conducted in the absence of any commercial or financial relationships that could be construed as a potential conflict of interest.

Publisher's Note: All claims expressed in this article are solely those of the authors and do not necessarily represent those of their affiliated organizations, or those of the publisher, the editors and the reviewers. Any product that may be evaluated in this article, or claim that may be made by its manufacturer, is not guaranteed or endorsed by the publisher.